SOME PERFORMANCE CHARACTERISTICS OF THE LRC $3\frac{3}{4}$-INCH PILOT EXPANSION TUBE USING AN UNHEATED HYDROGEN DRIVER

J. J. Jones

NASA Langley Research Center
Langley Station, Hampton, Va.

Presented at the Fourth Hypervelocity Techniques Symposium

Tullahoma, Tennessee
November 15-16, 1965

SOME PERFORMANCE CHARACTERISTICS OF THE LRC $3\frac{3}{4}$-INCH PILOT EXPANSION TUBE USING AN UNHEATED HYDROGEN DRIVER

J. J. Jones*

NASA Langley Research Center
Langley Station, Hampton, Va.

ABSTRACT

A former shock tunnel has been converted to expansion tube operation in order to study the expansion tube as a research tool and to compare its experimental performance to that predicted by previously performed theoretical calculations. This paper reports a portion of the overall evaluation program and is concerned only with expansion tube performance using a room-temperature hydrogen driver.

A microwave reflection technique has been used to supplement the usual pressure transducers, ion gaps, and collimated photomultipliers as a means of measuring velocity in the expansion tube. It has been found that the microwave signal detects the passage of the shock wave in the intermediate chamber and the helium-air interface in the acceleration chamber. The acceleration of the flow upon rupture of the secondary diaphragm is shown to occur in approximately $2\frac{1}{2}$ to 4 feet of travel, and the subsequent deceleration of the interface is small, averaging about 5 percent over the next 35 feet of travel.

Pitot pressures have been measured for a wide range of initial acceleration chamber pressure, thus corresponding to varying amounts of expansion of the shocked gas. The pitot pressures have been consistently less than predicted by theory. Correlation of the pitot pressure with wall static pressure and possible causes of the discrepancies are examined and discussed.

The rupture of the secondary diaphragm generates additional waves not considered in the elementary analysis, which assumes a diaphragm of negligible mass and overstrength. Consideration of possible ways to avoid this momentum loss from the flow has led to a study of the use of electromagnetic forces to open the diaphragm. Some results of a bench apparatus (no flow) are presented which show that with the expenditure of rather modest electrical energy a 1/64-inch-thick sheet-metal diaphragm will open to 6-inch diameter in 200 μsec or less.

---

*Supervisory Aerospace Engineer.

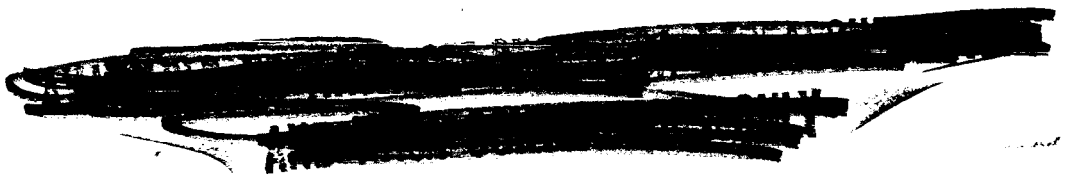

INTRODUCTION

The expansion tube has emerged as one possible solution to the problem of producing flows in the laboratory which are typical of reentry conditions while avoiding the problems associated with a stagnation region. In references 1 and 2 the theoretical performance of the expansion tube was presented. Since that time Langley Research Center has been engaged in a program to study the experimental performance of the expansion tube and to look for major differences between theory and experiment, which might be due to viscous effects, nonideal diaphragm rupture, finite chemical reaction rates, or three-dimensional flow effects, none of which were considered in the analytical work. A number of areas have been studied in this program including flow attenuation, secondary diaphragm rupture, flow turbulence, interface mixing, boundary-layer thickness, thermal nonequilibrium, and effective testing time. None of these problems has been answered completely but the experimental program to date has shown that the total influence of all these effects is not such as to seriously detract from the facility performance. A portion of this program is reported in the present paper, showing the instrumentation techniques being employed and the expansion tube performance in regard to flow velocity, static pressure, and test-section pitot pressure.

DESCRIPTION OF FACILITY

A former shock tunnel has been converted to expansion tube operation by the addition of a secondary diaphragm station and of a new model support section upstream of the nozzle. Figure 1 shows the facility schematically and indicates the pertinent dimensions. Because the present arrangement represents a conversion with minimum modification, the chambers do not have optimum length ratios. Two different locations have been used for the secondary diaphragm location, indicated as "A" and "B" on figure 1. The data presented in this paper were all obtained at location "B" which was 36 feet from the primary diaphragm. The removal of the throat insert converts the conical nozzle to a dump tank. The test section is of the "free jet" type consisting of a simple square cross-section box from which a model or probe can be supported and immersed in the flow issuing from the acceleration tube. The chambers are all $3\frac{3}{4}$ inches in diameter. Room-temperature hydrogen at approximately 100 atmospheres pressure was used as the driver in the present experiments. The test gas was room air and helium was used as the acceleration chamber gas after first evacuating the acceleration chamber and dump tank to approximately 10^{-4} torr. The primary diaphragm was steel, the secondary diaphragm was 1/4 mil mylar.

The velocity of the shock waves and interface were measured with the aid of ion gaps, photomultipliers, and pressure transducers stationed in the wall of chambers as shown, as well as a microwave signal introduced through an antenna located downstream of the test section.

RESULTS

Flow-Velocity Measurements

The microwave signal reflects off the shock wave during its traverse of the test gas chamber as verified by the ion gap signals (see fig. 2). The resulting histories of shock attenuation are in essential agreement with earlier attenuation studies made in this facility and reported in reference 3. The shock wave decays approximately 6 percent in traveling the 36-foot-long test gas chamber.

After rupture of the secondary diaphragm the helium-air interface has been found to be the reflecting surface for the microwave signal. Figure 2 illustrates that the microwave signal is in agreement with the interface position as determined by the photomultipliers and pitot pressure probe. The helium shock detection is provided by static pressure transducers mounted in the acceleration tube wall.

Figure 3 presents the interface velocity for several values of p_{10}. The initial test gas chamber pressure p_1 was 22 torr for all runs shown. It may be seen that the interface reaches it maximum velocity in $2\frac{1}{2}$ feet $\left(x = 38\frac{1}{2} \text{ ft}\right)$ to 4 feet (x = 40 ft) of travel and the subsequent decay is small, particularly for the higher velocity conditions. The helium shock velocity has not been obtained with comparable precision, since pressure transducers were located at not more than four stations, but it appears that the shock attenuation was somewhat greater than that shown for the interface.

Static-Pressure Measurements

Figure 4 presents the measured static pressure p_5 as a function of the measured interface velocity V_I. For all runs shown the initial test gas chamber pressure was 22 torr and thus the initial shock velocity was essentially the same, 9450 ft/sec $\pm$ 4 percent. The flow velocity was varied by varying the initial acceleration chamber pressure p_{10} over the range 10^{-2} to 2 torr. The data show a tendency to show a somewhat lower pressure than equilibrium theory for a given velocity. The "frozen" theoretical curve shown is based on the assumption that dissociation and vibration energy are frozen at their equilibrium levels behind the primary shock wave. The data are seen to be bracketed by the

two extremes of equilibrium and "frozen" flow. However another possible effect is indicated on the figure. The interface was observed to slow down by as much as 1000 ft/sec during its traverse of the acceleration tube. The mechanism for this velocity reduction is presumably downstream facing expansion waves, generated by the growing boundary layer in the flow upstream. Figure 4 also presents a theoretical calculation which includes the effect of downstream expansions sufficient to reduce the flow velocity by 1000 ft/sec. Thermal equilibrium was assumed throughout for this calculation. It is seen that the data are largely bracketed by this curve and the equilibrium expansion calculation, and that a better fit would have been obtained with a less severe attenuation assumption, perhaps $\Delta V = -500$ ft/sec.

Pitot-Pressure Measurements

A pitot probe has been mounted on or near the tube center line at the test-section location. Figure 5 shows the general nature of the records obtained. The oscillograph displays an electronically filtered record as well as an unfiltered trace. The rapid rise of the pitot pressure upon arrival of the interface is noteworthy. This rapid rise is an indication that diffusion at the interface is not severe.

The effect of varying the amount the test gas expands (i.e., varying p_{10}) is shown on figure 6, where several typical pitot-pressure traces are shown. At high values of p_{10} a dip in the pitot pressure occurs shortly after the interface arrives. As the pressure is reduced the dip becomes less evident, either disappearing or is masked in the rising pitot pressure due to the fan arrival. The calculated arrival time of the tail of the expansion is indicated on each trace of figure 6. The origin of this pressure dip is not clear as yet. Studies have indicated that it is not due to acceleration effects on the transducer, gage heating, pitot probe design, or type of transducer used, so it has been concluded that it is aerodynamic in nature. Increasing the secondary diaphragm mass or burst strength has only small effect on the pitot-pressure record. If the dip is the result of the arrival of a downstream facing expansion wave generated by some upstream source, then the wave arrival should be evident to at least the same degree in the static-pressure records. On some runs a slight decrease in static pressure has been noted but it does not appear sufficient to support this hypothesis. Other possible causes of the pitot-pressure dip are currently under investigation.

Figure 7 shows the correlation of the measured pitot pressures (prior to the arrival of the dip, where observed) with the calculated curves considered previously. The measured values fall below the calculated values. Perhaps the best agreement is obtained with the curve which considers the loss in velocity due to the attenuation waves, but a loss of 1000 ft/sec is required to correlate the pitot-pressure data, and this is inconsistent with the static-pressure data. It should be

noted that flow nonequilibrium, as indicated by the extreme "frozen" case, is a less satisfactory correlation.

Flow Turbulence

A matter of some concern in the successful operation of the expansion tube is the level of flow turbulence which is encountered in the test flow, since past experience in shock tubes has shown the flow behind the interface to be highly turbulent in nature. No direct studies of turbulence have been made in the present program, but the observed oscillations or "ringing" of the pitot pressure transducer at or near its natural frequency has been assumed to be due to flow turbulence, and therefore it is of interest to attempt to use the transducer ringing as an indication of turbulent noise. Figure 8(a) shows an unfiltered pilot-pressure trace on an expansion tube run. Figure 8(b) is a corresponding pitot-pressure record in the same facility operated as a shock tube. The shock tube condition was selected to obtain approximately the same value of pitot pressure. The free-stream unit Reynolds numbers of the two flows were also approximately equal. The expansion tube record displays two distinct levels of noise, which is typical of most runs. For the early part of the airflow the amplitude of the oscillation is certainly no worse than the shock tube flow. Later, however, a sudden increase in the amplitude is observed. It should be noted that a nearby wall static pressure also shows this increased noise at essentially the same instant. Boundary-layer transition is currently being investigated as a possible cause of the increased noise level. It should be pointed out that any conclusions drawn from the comparison of amplitudes of transducer noise must be narrowly qualified, even assuming that the driving potential is flow turbulence, since presumably the transducer's resonance will couple only with a small range of the frequency spectrum of the turbulence and is not necessarily a true indication of overall turbulence level.

Secondary Diaphragm Rupture

It was shown in reference 4 that finite mass and strength of the secondary diaphragm can produce rather large disturbances in the flow. The flow in the intermediate chamber, which for expansion tube operation is the test gas, is acted on by an upstream facing shock wave produced by the finite time required to rupture and accelerate the diaphragm. It is of interest therefore to investigate practical methods of rupturing the diaphragm with external forces, possibly just prior to shock arrival.

For this purpose an exploratory study has been made of the use of electromagnetic forces to rupture and open thin sheet-metal diaphragms. In this study, which has been conducted on a small bench-type no-flow apparatus, a single turn coil was placed on close proximity but not in electrical contact with the diaphragm, which had been prescribed with two scribes in the conventional manner. If applied to the expansion

tube, the coil is envisioned as potted into the wall of the tube, with its axis coincident with the tube axis, on the upstream side of the diaphragm. A schematic drawing of the arrangement is shown in figure 9.

The diaphragm was ruptured by discharging the energy stored in an 860-microfarad capacitor bank into the coil. The circuit had a ringing frequency of approximately 16 kilocycles and a decay time constant of about 130 microseconds. Note that the diaphragm was not retained at the inner diameter of the coil, corresponding to the internal diameter of the tube. A drastic reduction in opening force was observed when the diameter of the retaining flange was reduced in this manner. The expected magnetic pressure distribution is shown in figure 9. Note that the region of high load on the diaphragm is removed if the diaphragm is retained opposite the coil.

Figure 10 shows a photograph of a ruptured 0.016-inch-thick aluminum diaphragm. The diaphragm had been prescribed to a depth of 0.008 inch. The manner in which the tabs are folded, with the tips tucked under, is typical.

The opening times of the diaphragm were measured with an optical arrangement in which the amount of light falling on a photo cell was proportional to the open area of the diaphragm. Data on typical opening times are shown in figure 11. These data are shown on the basis of time to 3/4 of full open because of the asymptotic manner in which complete opening was approached. Aluminum and copper diaphragms have been used ranging in thickness from 0.003 to 0.032 inch. Optimum opening times appear to result when the diaphragms are 0.016 to 0.020 inch thick, which is the order of one characteristic skin depth for the circuit frequency. This investigation has been exploratory in nature and it is anticipated that improvements in opening time and configuration will result from a more detailed study.

CONCLUSIONS

An experimental study of expansion tube performance using a room-temperature hydrogen driver has shown that in a number of important aspects the differences from one-dimensional inviscid calculation are moderate and tolerable.

A microwave reflection technique has been shown to permit measurement of the velocity of the test flow, and indicates that the attenuation is of the order of 5 percent or less over a distance of about 35 feet (110 tube diameters). The static pressure was shown to be slightly less than equilibrium calculation, but inclusion of a downstream wave family which produces a 500 ft/sec attenuation in flow velocity would correlate the static pressure assuming local equilibrium. The pitot pressure has shown a tendency to be lower than the corresponding calculated values for static pressure and would require about

1000 ft/sec attenuation to correlate, which was more than observed on most runs. In addition a dip in the pitot pressure was noted when the facility was run in the underexpanded case. However the dip did not occur during the test period for more fully expanded cases. The oscillations of the pitot pressure transducer were of the same order of magnitude during the expansion tube test period as for a similar pitot pressure behind a shock wave. This was taken to be at least some indication that the flow turbulence level was not necessarily greater than presently experienced in shock tube flows.

Consideration of ways to avoid the use of flow momentum to rupture the secondary diaphragm has led to a study of electromagnetic diaphragm ruptures. Exploratory tests have shown that a 1/64-inch-thick sheet-metal diaphragm will open to 6 inches diameter in 200 microseconds or less.

SYMBOLS

p_1	initial test gas pressure
p_{10}	initial pressure in acceleration chamber
p_5	static pressure in flowing test gas
P_T	test-section pitot pressure
V_I	velocity of acceleration gas - test gas interference
X	distance downstream from primary diaphragm

REFERENCES

1. Trimpi, Robert L.: A Preliminary Theoretical Study of the Expansion Tube, a New Device for Producing High-Enthalpy Short-Duration Hypersonic Gas Flows. NASA TR R-133, 1962.

2. Trimpi, Robert L.: A Preliminary Study of a New Device for Producing High Enthalpy Short Duration Gas Flows. Second National Hypervelocity Techniques Symposium, Mar. 19-20, 1962.

3. Jones, Jim J.: Experimental Investigation of Attenuation of Strong Shock Waves in a Shock Tube with Hydrogen and Helium as Driver Gases. NACA TN 4072, 1957.

4. Knoos, Stellan: A Theoretical and Experimental Study of the Opening Time of the Low Pressure Diaphragm in a Double-Diaphragm Shock Tube. Royal Institute of Technology, Stockholm, Aug. 1963.

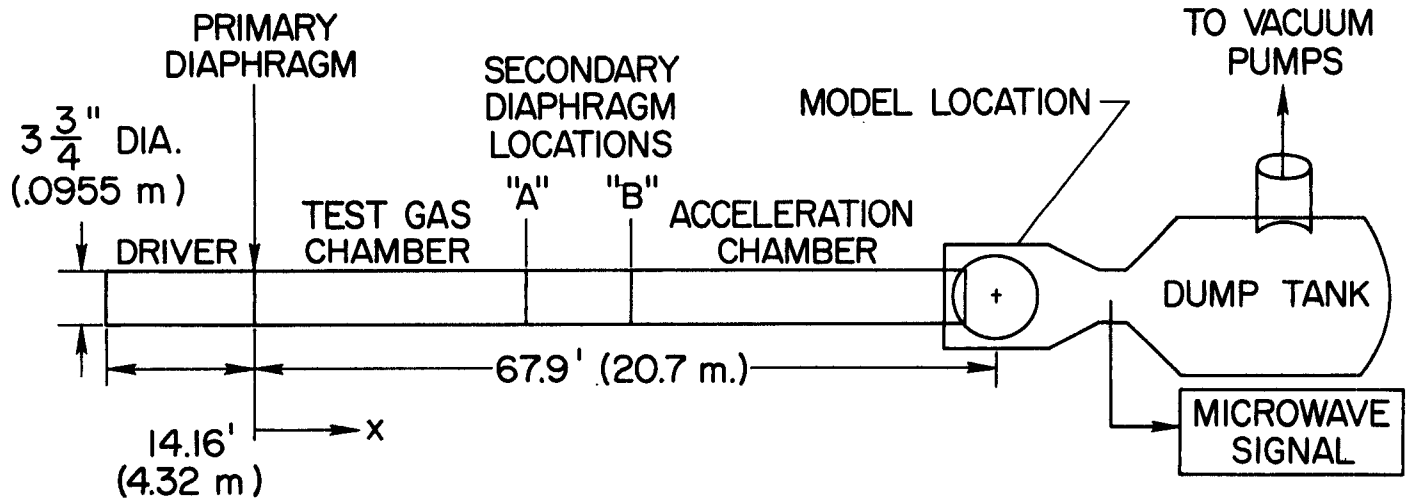

NASA

Figure 1.- Sketch of Langley Pilot Model Expansion Tube.

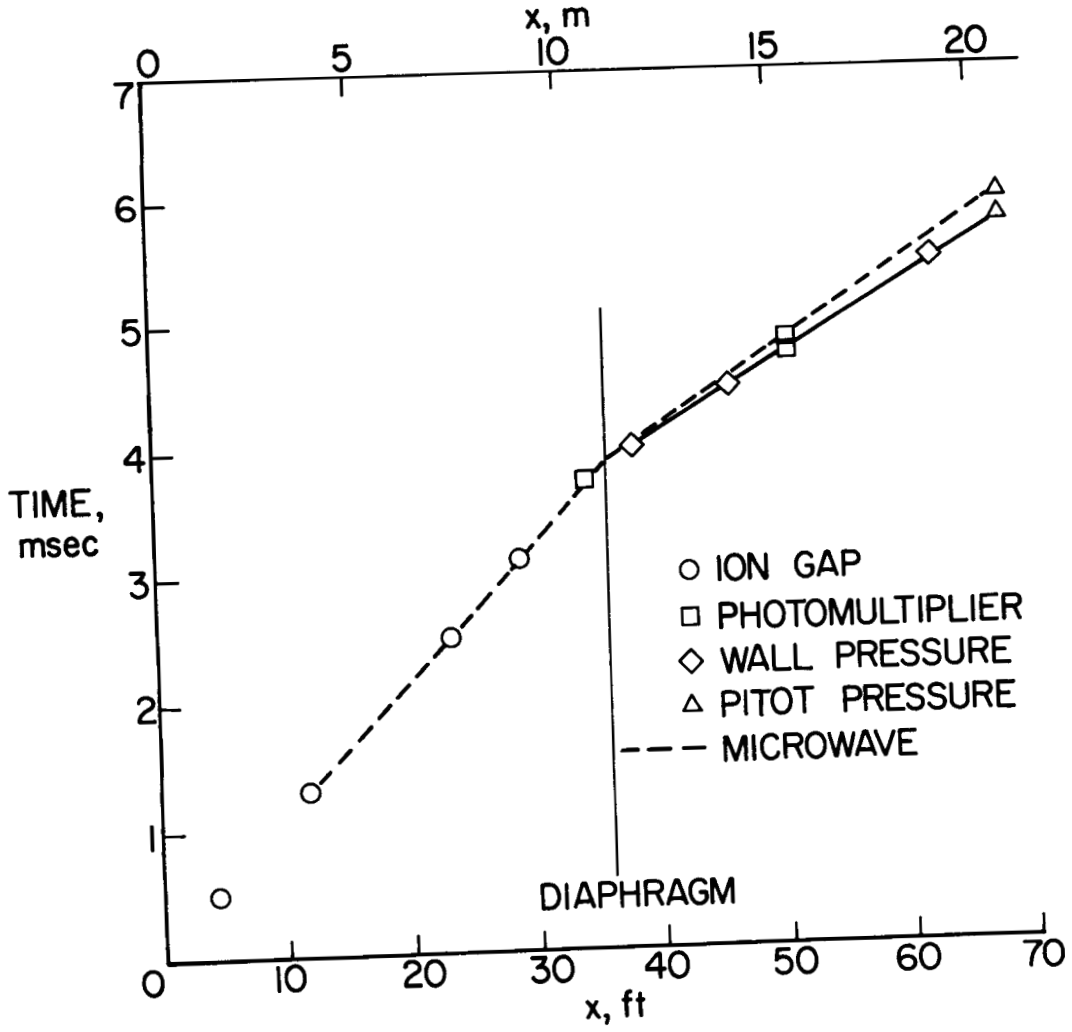

NASA

Figure 2.- Example of distance time diagram showing correspondence of microwave signal with other wave-detection instrumentation.

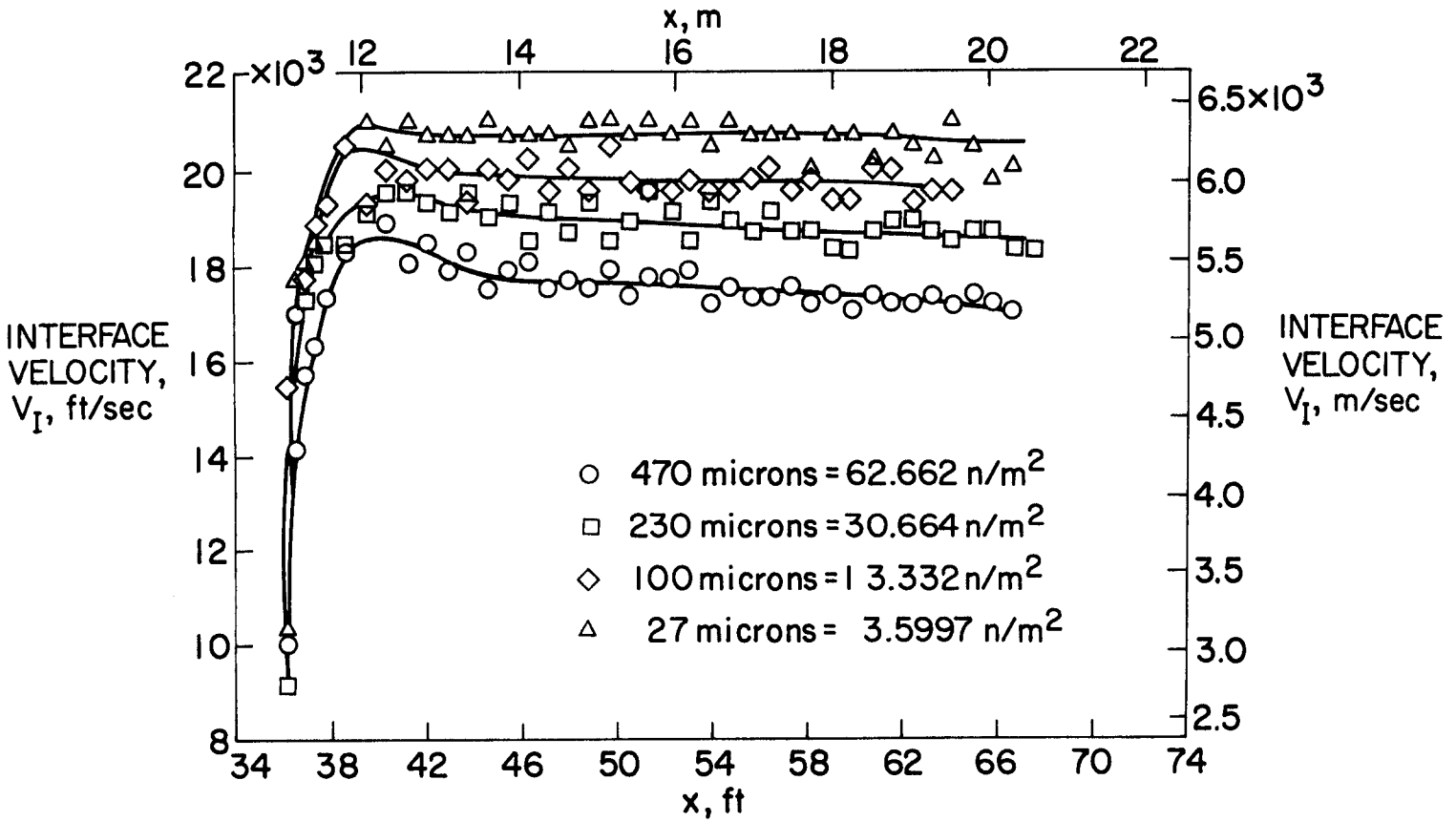

NASA

Figure 3.- Interface velocity as determined by microwave signal for several values of p_{10}. p_1 = 22 torr = 2933 n/m².

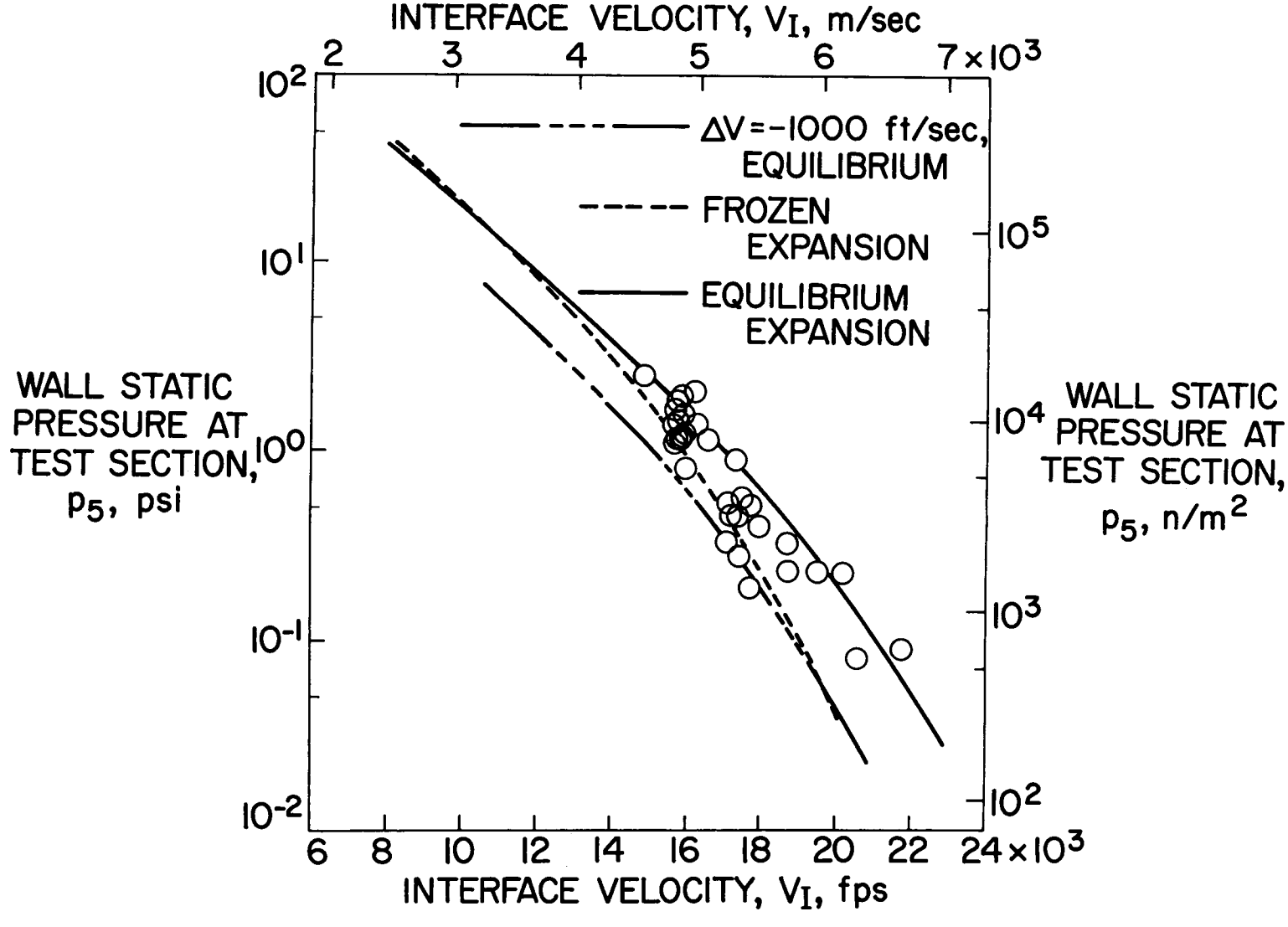

NASA

Figure 4.- Wall static pressure at test section - experiment compared with several theoretical assumptions. p_1 = 22 torr = 2933 n/m^2.

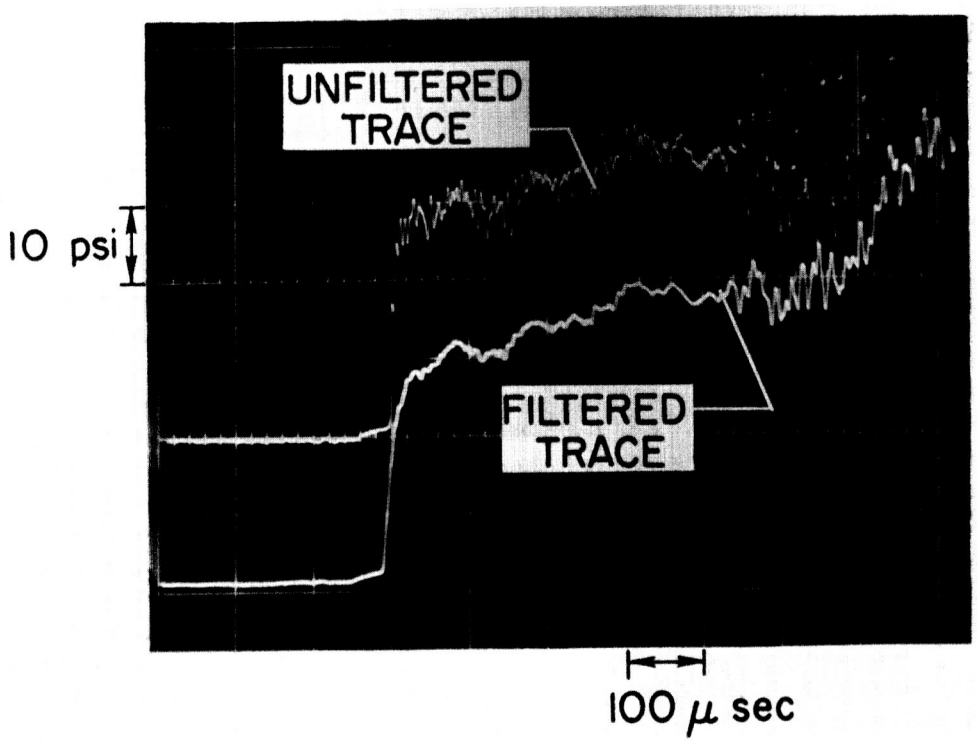

NASA

Figure 5.- Sample pitot pressure record.

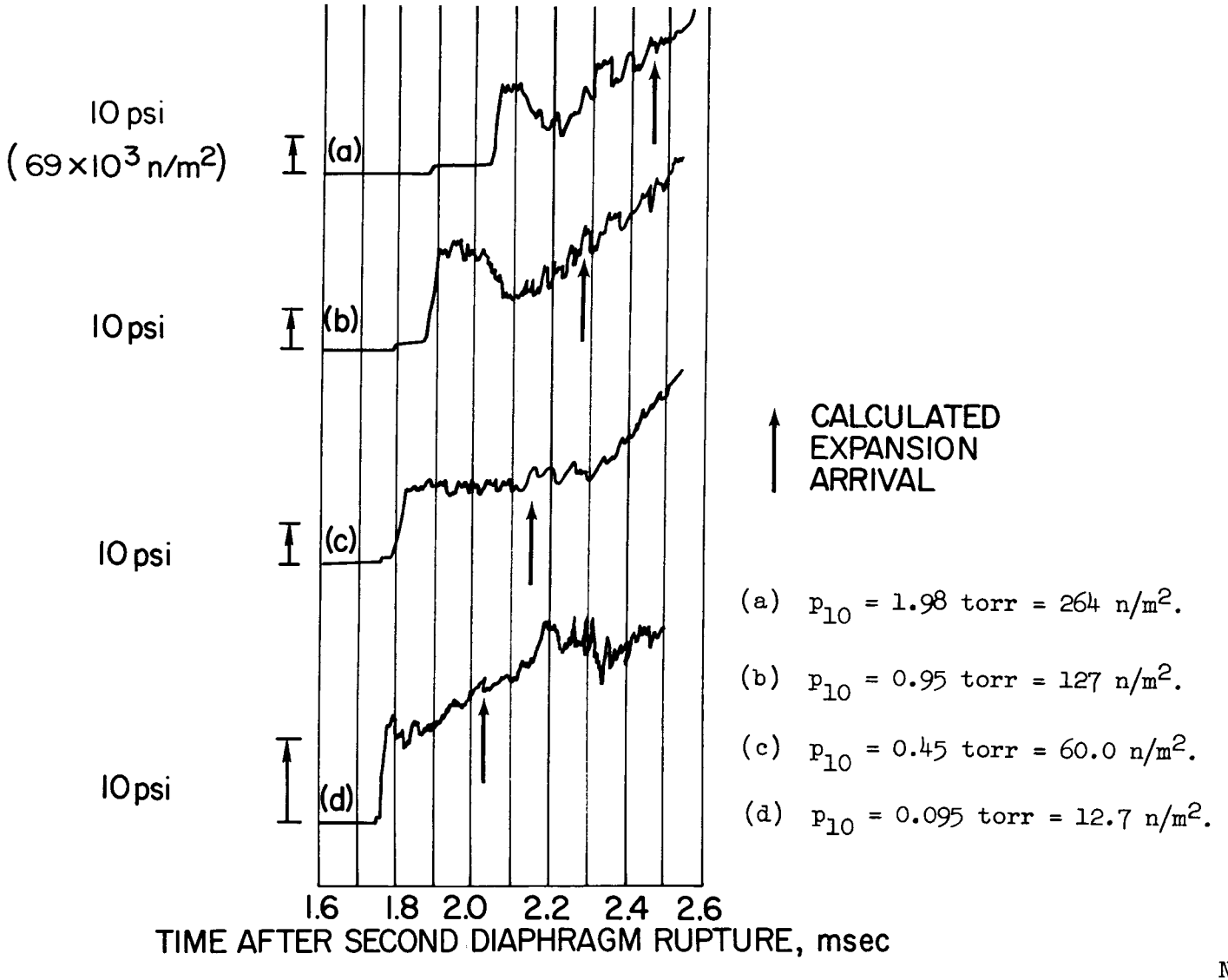

NASA

Figure 6.- Pitot pressure tracings showing effect of varying acceleration chamber pressure p_{10}.

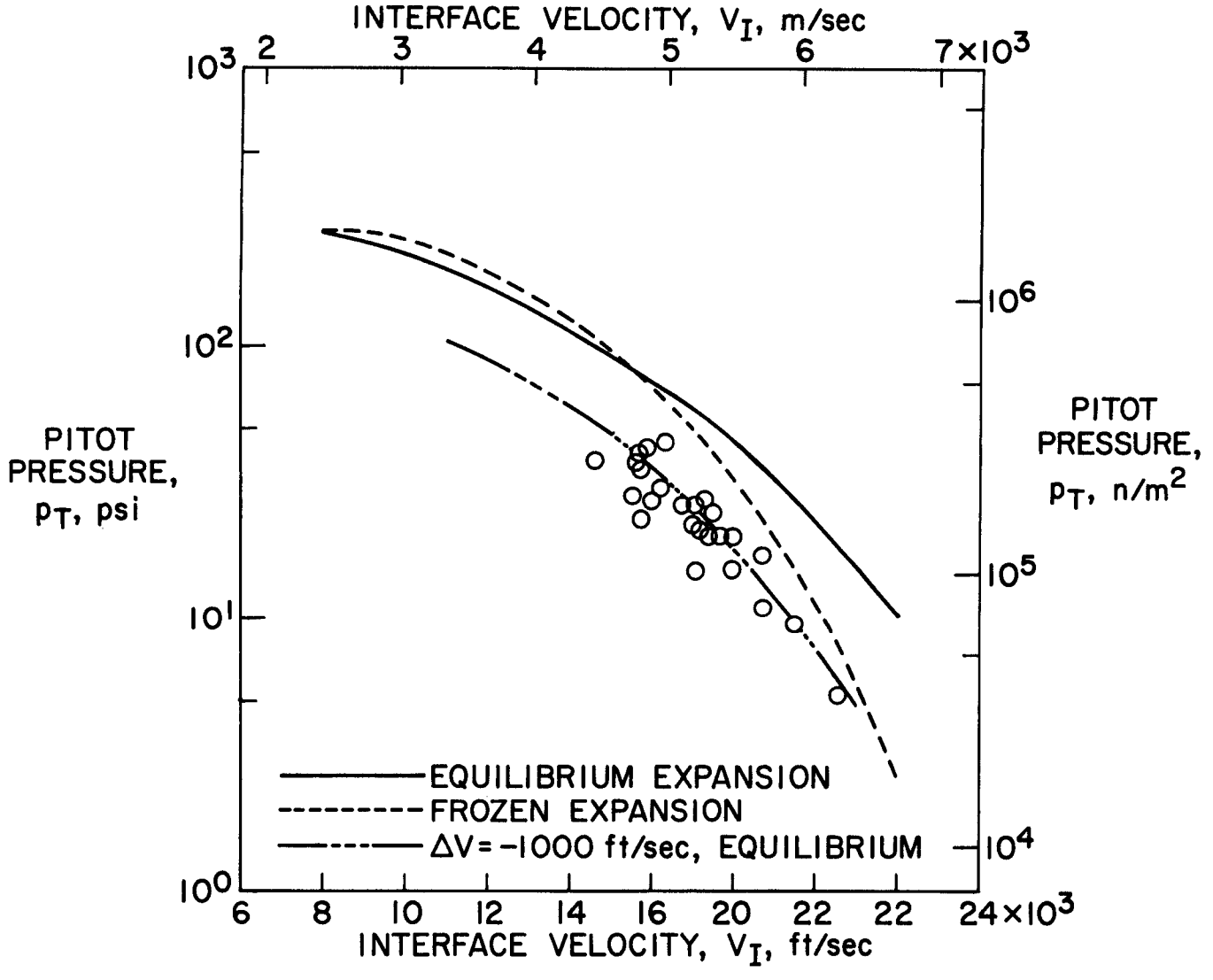

NASA

Figure 7.- Comparison of calculated and measured pitot pressures. p_1 = 22 torr = 2933 n/m^2.

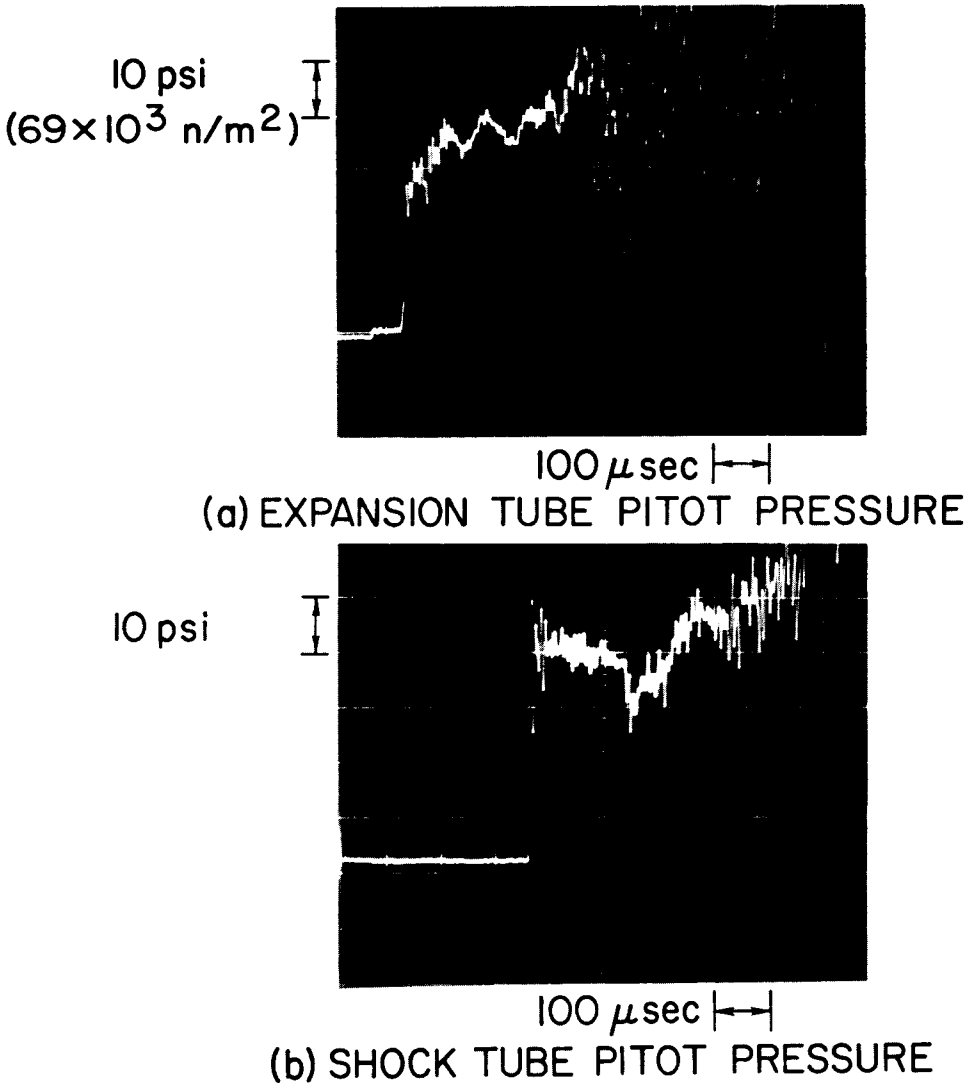

NASA

Figure 8.- Comparison of noise induced on pitot pressure transducer in expansion tube and shock tube flows.

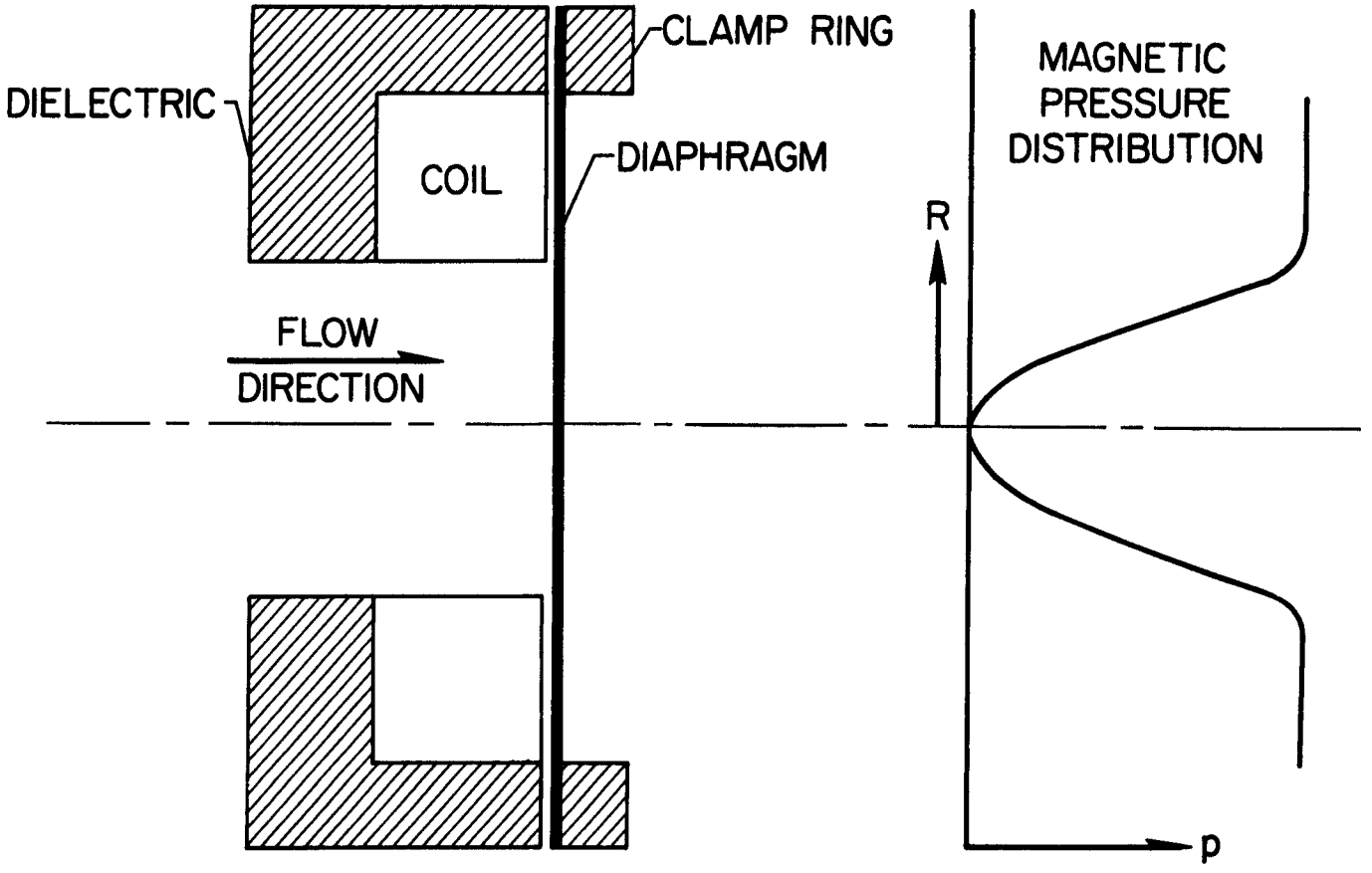

NASA

Figure 9.- Sketch of coil arrangement.

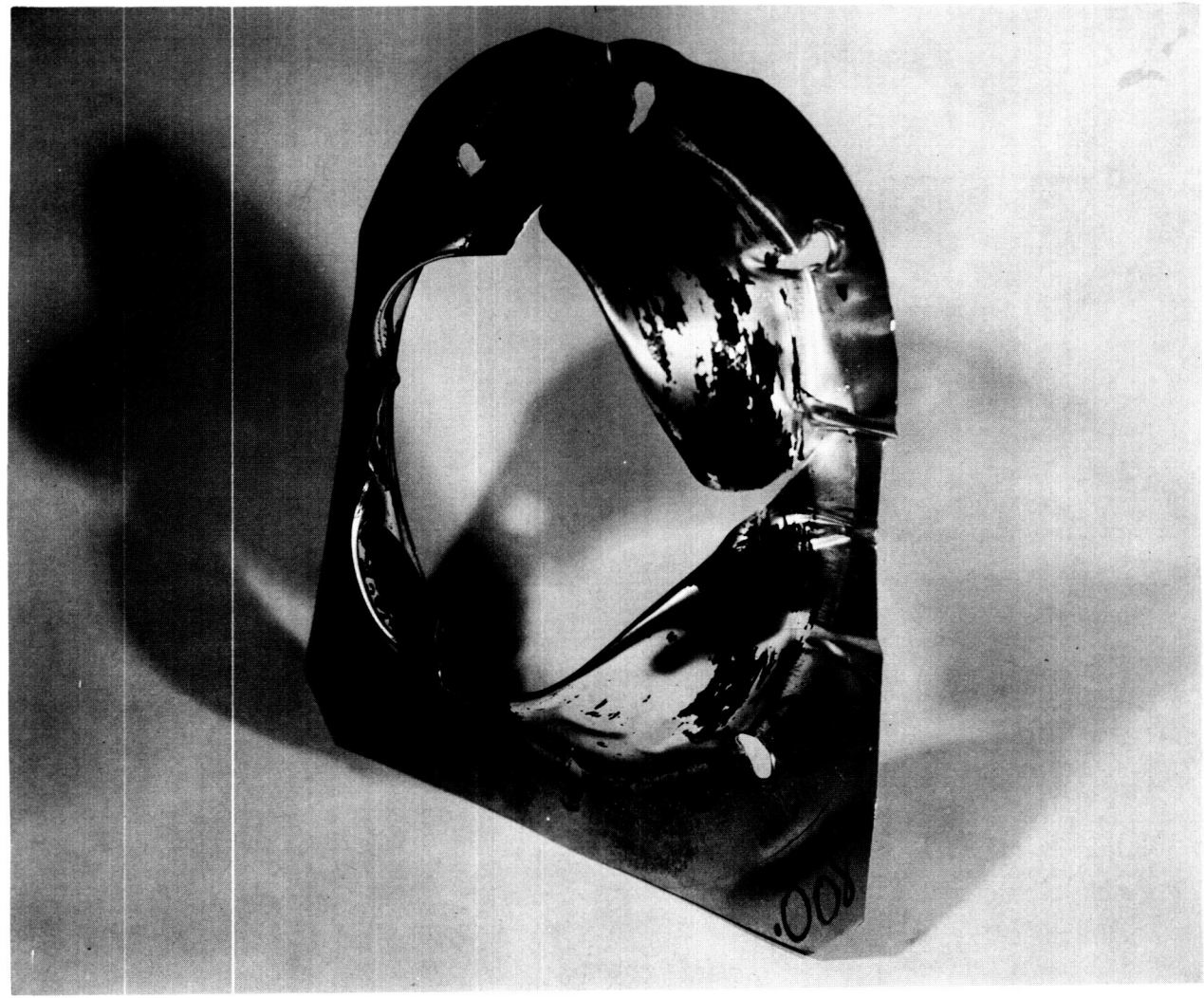

NASA

Figure 10.- Sample diaphragm ruptured by coil.

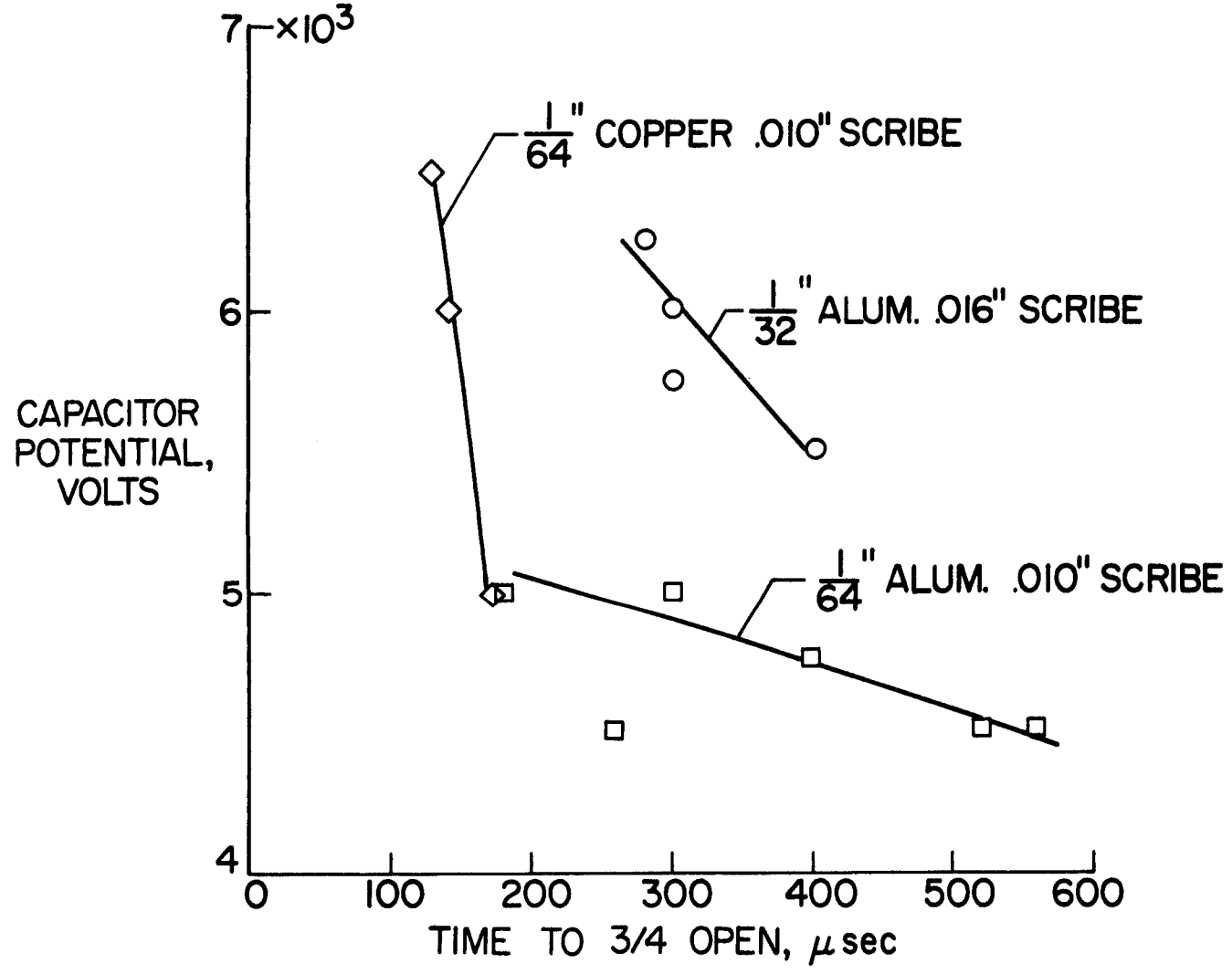

NASA

Figure 11.- Diaphragm opening times.